INT. J. GEOGRAPHICAL INFORMATION SYSTEMS, 1996, VOL. 10, NO. 5, 629–641

Research Article

Modelling topographic potential for erosion and deposition using GIS

HELENA MITASOVA

U.S. Army Construction Engineering Research Laboratories, P.O. Box 9005, Champaign, Illinois 61826-9005, U.S.A. and Department of Geography, University of Illinois at Urbana-Champaign, Urbana, Illinois 61801, U.S.A.

JAROSLAV HOFIERKA, MAROS ZLOCHA

Faculty of Natural Sciences, Comenius University, Mlynska dolina, 84215 Bratislava, Slovakia.

and LOUIS R. IVERSON†

Illinois Natural History Survey, Champaign, Illinois 61820, U.S.A.

(*Received 5 May 1993; accepted 16 January 1995*)

Abstract. Modelling of erosion and deposition in complex terrain within a geographical information system (GIS) requires a high resolution digital elevation model (DEM), reliable estimation of topographic parameters, and formulation of erosion models adequate for digital representation of spatially distributed parameters. Regularized spline with tension was integrated within a GIS for computation of DEMs and topographic parameters from digitized contours or other point elevation data. For construction of flow lines and computation of upslope contributing areas an algorithm based on vector-grid approach was developed. The spatial distribution of areas with topographic potential for erosion or deposition was then modelled using the approach based on the unit stream power and directional derivatives of surface representing the sediment transport capacity. The methods presented are illustrated on study areas in central Illinois and the Yakima Ridge, Washington.

1. Introduction

Several erosion models have already been interfaced with GIS, including various modifications of an empirical model represented by the Universal Soil Loss Equation (USLE) (e.g., Warren *et al.* 1989, Flacke *et al.* 1990, Huang and Ferng 1990), and watershed models for non-point source pollution such as AGNPS or ANSWERS (de Roo *et al.* 1989, Rewerts and Engel 1991, Srinivasan and Engel 1991). The USLE was originally developed for agricultural fields and its application to landscape scale erosion modelling is often inappropriate (Foster and Wischmeier 1974, Moore and Wilson 1992). Recently developed models based on the unit stream power theory (Moore and Burch 1986 b, Moore and Wilson 1992, Mitasova and Iverson 1992, Hofierka 1992) include the influence of terrain shape and are therefore more suitable for complex topographic conditions. However, their use within a GIS requires a high resolution DEM and reliable tools for topographic analysis.

† Present address: U.S. Forest Service, 359 Main Road, Delaware, Ohio 43015, U.S.A.

0269–3798/95 $12.00

Although topographic analysis is a common part of currently used GIS, the methods used for computation of DEM and topographic parameters (see e.g., Douglas 1986, Pike 1993) do not always fulfill the requirements for physically based erosion modelling. Resolution and accuracy of available DEMs makes the flow tracing difficult because of insufficient vertical resolution and the incidence of numerous pits that trap the flow lines (Jenson and Domingue 1988, Martz and Garbrecht 1992). Standard algorithms for flow tracing, which use only a limited number of flow directions (most often 8) from each grid cell can lead to various unrealistic situations, such as prevailing flow in the direction parallel to x or y axes or diagonals (Fairfield and Leymarie 1991). Recently, significant improvements in the computation of DEMs from digitized contours were achieved by applying the spline function with drainage enforcement (Hutchinson 1989) and by the computation of DEMs using the regularized spline with tunable tension and smoothing (Mitasova and Mitas 1993, Mitasova and Hofierka 1993, Mitasova *et al.* 1995). Several new algorithms for flow tracing help to overcome deficiencies of standard algorithms by using the random-eight node approach (Fairfield and Leymarie 1991), multiple nearest neighbour nodes (Freeman 1991), and by using 360 directions of flow with the vector-grid algorithm (Mitasova and Hofierka 1993, Mitasova *et al.* 1995).

The aim of this study is to develop methods for computation of topographic factors both for the standard USLE and for the unit stream power based model suitable for complex terrain and applicable to large areas. Special attention is given to the proper representation of terrain and computation of topographic parameters significant for erosion/deposition modelling. In the next section, topographic factors for erosion models are discussed and the approach for the estimation of erosion and deposition is derived. Then, improved methods for the computation of topographic parameters within GIS are presented and examples of applications are given. The regularized spline with tension used for interpolation and estimation of derivatives is briefly described in the Appendix.

2. Topographic factors for erosion models

2.1. *LS factor in the Universal Soil Loss Equation*

The Universal Soil Loss Equation (USLE) is an empirical equation designed for the computation of soil loss in agricultural fields. Various modifications of this equation are often applied to the estimation of soil loss using GIS. The influence of terrain on erosion is represented by the *LS* factor which reflects the fact that erosion increases with slope angle and slope length. The *LS* factor is computed as (Wischmeier and Smith 1978)

$$LS = (\lambda/22{\cdot}13)^t \cdot (65{\cdot}4 \sin^2 \beta + 4{\cdot}56 \sin \beta + 0{\cdot}0654) \quad (1)$$

where λ is the horizontal projection of slope length [m], t is the constant dependent on the value of slope and β is the slope angle [deg]. The topographic factor for USLE has been recently improved by incorporation of the influence of profile convexity/concavity using segmentation of irregular slopes and by improving the empirical equations for the computation of *LS* factor (Foster and Wischmeier 1974, Renard *et al.* 1991) as a part of the Revised Universal Soil Loss Equation (RUSLE).

Both USLE and RUSLE consider erosion only along the flow line without the influence of flow convergence/divergence and the equations can be properly applied only to areas experiencing net erosion. Depositional areas should be excluded from

the study area. Therefore, direct application of USLE to complex terrain within GIS is rather restricted.

2.2. *Topographic factor based on the unit stream power*

By analysing several currently used erosion models and sediment flux equations, Moore and Wilson (1992) have shown that the general form of the sediment transport equation can be used to describe the effects of terrain on soil erosion. The general equation (Julien and Simons 1985) has the following form

$$q_s = \phi q^m (\sin\beta)^n i^\delta \left(1 - \frac{\tau_0}{\tau}\right)^\varepsilon \tag{2}$$

where q_s is the sediment flux [$\mathrm{kg\,m^{-1}\,s^{-1}}$], q is the water flux [$\mathrm{m^3\,m^{-1}\,s^{-1}}$], β is the slope angle, i is the rainfall intensity [$\mathrm{m\,s^{-1}}$], τ_0, τ are the critical shear stress and shear stress [Pa] respectively, and $\phi, m, n, \delta, \varepsilon$ are experimental or physically based coefficients.

In the sediment transport equation, the influence of terrain is incorporated in the term $q^m(\sin\beta)^n$. If we assume uniform rainfall excess and steady state overland flow then the water flux q can be expressed as

$$q = Ai_e \tag{3}$$

where A is the upslope contributing area per unit contour width [$\mathrm{m^2\,m^{-1}}$] and i_e is the rainfall excess rate [$\mathrm{m\,s^{-1}}$] (Moore and Burch 1986 a). The equation representing the influence of terrain on soil erosion can then be rewritten in dimensionless form so that the dimensionless index of sediment transport capacity T becomes unity for the case when the upslope contributing area $A = 22{\cdot}13$ [$\mathrm{m^2\,m^{-1}}$], and the slope is 9 per cent.

$$T = \left(\frac{A}{22{\cdot}13}\right)^m \left(\frac{\sin\beta}{0{\cdot}0896}\right)^n \tag{4}$$

which is the unit stream power based LS factor proposed by Moore and Burch (1986 a). It has been shown that the values of $m = 0{\cdot}6$, $n = 1{\cdot}3$ give results consistent with RUSLE LS factor for the slope lengths $\lambda < 100$ m and the slope angles $\beta < 14°$ (Moore and Wilson 1992).

Moore and Burch (1986 b) and Moore and Wilson (1992) have proposed to measure the potential of landscape for erosion or deposition by a topographic index representing the change in sediment transport capacity in the direction of flow $E = dT/ds$. As a refined technique to compute E we propose to use continuous representation of sediment transport capacity and calculate directly its derivative, instead of using the originally suggested finite difference approach. Thus the spatial distribution of sediment transport capacity T given by the equation (4) is represented by a bivariate continuous function

$$T = g(x, y) \tag{5}$$

where (x, y) are the georeferenced coordinates and $g(x, y)$ is in our case the spline function applied to grid representing T. The change in the sediment transport capacity in the direction of flow is then expressed by a directional derivative:

$$E = \frac{dT}{ds} = g_x \cos\alpha + g_y \sin\alpha \tag{6}$$

where $g_x = \partial T/\partial x$, $g_y = \partial T/\partial y$ are the partial derivatives of function representing T, and α is the aspect angle computed from elevation surface. The index E is positive for areas with topographic potential for deposition where the sediment transport capacity decreases, and negative for areas with erosion potential where the sediment transport capacity increases. While the directional derivative accounts for acceleration in the direction of terrain gradient the acceleration in the direction perpendicular to gradient is neglected. Therefore the flow convergence/divergence is incorporated only through upslope contributing area and the approach does not model the full effect of two-dimensional flow.

3. Topographic analysis

The erosion models described in the previous section were implemented within GIS using spline interpolation and a vector-grid approach to flow tracing. Computation of slope, aspect, slope length, or upslope contributing area is based on the representation of terrain by a continuous bi-variate function

$$z = f(x, y) \tag{7}$$

computed from digitized contours, direct field measurements of elevations, or other digital elevation data. In our implementation, regularized thin plate spline with tension and smoothing (Mitasova and Mitas 1993, Mitasova and Hofierka 1993) was used (Appendix). This function was specially designed to fulfill the requirements of topographic analysis. By tuning the tension and smoothing parameters it is possible to minimize the overshoots, artificial pits or banding effect of the elevation values around the contours, observed for the less general forms of splines such as the thin plate spline (see e.g., example in Mitasova and Mitas 1993). GIS implementation of this function provides several tools for controlling the quality of resulting DEMs, such as computation of deviations, predictive errors based on ordinary crossvalidation procedure, and computation of curvatures useful for detecting artificial waves around contours caused by improperly chosen tension parameter. Regular derivatives of all orders make the interpolation function suitable for direct computing of topographic parameters such as slope, aspect, and curvatures. This approach increases the accuracy and reliability of topographic analysis when compared to the standard local polynomial interpolation from 3 by 3 neighbourhood applied to grid DEM, as demonstrated by Mitasova (1985), Mitasova *et al.* (1995).

Using the partial derivatives of regularized spline with tension, *slope* is computed from the gradient $\nabla f = (f_x, f_y)$ of elevation surface as

$$\tan\beta = \sqrt{f_x^2 + f_y^2} \tag{8}$$

where β is the slope angle [deg], and f_x, f_y are the first order partial derivatives of function given by equation (7). *Aspect* controls the direction of flow, and is necessary for the computation of upslope contributing areas and for the directional derivatives in equation (6). It is given by the direction of minus gradient

$$\tan\alpha = \frac{-f_y}{-f_x} \tag{9}$$

where α is the aspect angle [deg].

Upslope contributing area is the area from which the water flows into a given grid cell. It is used as a measure of water flux in equation (4). Upslope contributing area per unit contour width A_j for the given grid cell j is computed from the sum

of grid cells from which the water flows into the cell j

$$A_j = \frac{1}{b} \sum_{i=1}^{n_j} \mu_i a_i \tag{10}$$

where a_i is the area of grid cell, n_j is the number of cells draining into the grid cell j, μ_i is the weight depending on the run-off generation mechanism and infiltration rates, and b is the contour width approximated by the cell resolution. This approximation is acceptable if the DEM is interpolated with the adequate resolution which depends on the curvature of terrain surface. Our experience, supported by several recent studies (e.g., Zhang and Montgomery 1994) is that the resolution $2m - 20m$ is appropriate for models using upslope contributing areas in regions with complex terrain. In this study we assume $\mu = 1$ and $a_i = b$ by $b = \text{const.}$, so the upslope contributing area is simply $A_j = n_j \times b$.

For the computation of number of cells n_j draining into each grid cell flow lines are constructed *downhill* from each grid cell until they reach a cell with slope lower than the specified minimum, boundary line, singular point, or barrier (e.g., road). An improved algorithm for the construction of flow lines based on vector-grid approach (Mitasova and Hofierka 1993) is used. Flow lines constructed by this algorithm are represented in vector format. The points defining the flow line are computed as the points of intersection of a line constructed in the flow direction given by aspect angle α and a grid cell edge. Downhill flow lines merge in valleys (figure 1) and they can be used also for the extraction of channels (Jenson and Domingue 1988, Gardner *et al.* 1990, Qian *et al.* 1990).

Flow path length is used in the standard form of USLE/RUSLE and is appropriate for hillslopes with negligible water flow convergence/divergence. For the computation of flow path length flow lines are generated *uphill* from each grid cell in the gradient direction ($\alpha + 180°$) until they reach a grid cell with the slope lower than the specified minimum, boundary line, singular point or barrier. Flow path length λ_j for each j-th grid cell is then computed from the coordinates of points (x_i, y_i); $i = 1, \ldots n$ of their intersection with grid cells

$$\lambda_j = \sum_{i=1}^{n} \sqrt{(x_{i+1} - x_i)^2 + (y_{i+1} - y_i)^2} \tag{11}$$

Uphill flow lines merge on ridge lines (figure 2). By redirecting the order of points defining the flow line, dispersed water flow can be simulated.

4. Examples of application

The approach to the modelling of topographic potential for erosion and deposition presented above is illustrated using two examples with different original elevation data. The first one is a small region (500 m by 500 m) in Central Illinois and uses digitized contours. The region is within the construction area of a proposed water reservoir and the results presented here are part of the study on the environmental impact of this reservoir (Mitasova and Iverson 1992). The second example is a 3·6 km by 4 km region in the Yakima Ridge, Washington and uses standard USGS 30 m DEM. The analysis was performed for the project on modelling of complex ecosystems.

The proposed methods and algorithms were implemented within GRASS GIS (GRASS4.1 Reference Manual 1993) as commands *s.surf.tps* for interpolation and topographic analysis and *r.flow* for the construction of flow lines and computation

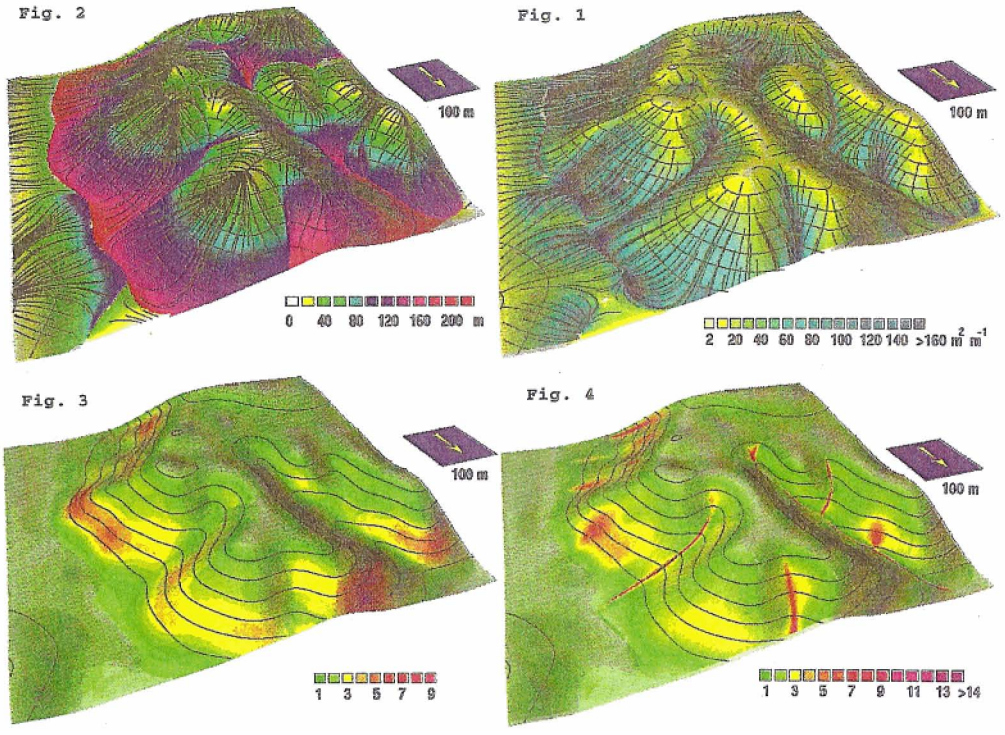

Figure 1. Flow lines constructed downhill, merging in valleys. Colour represents the values of upslope contributing areas.

Figure 2. Flow lines constructed uphill, merging in ridges. Colour represents the values of flow path length.

Figure 3. *LS* factor for the Universal Soil Loss Equation.

Figure 4. Sediment transport capacity index.

of flow path lengths and upslope contributing areas. Topographic factors for erosion models were computed using the raster map calculator *r.mapcalc*. The results of analysis and modelling were visualized using the GRASS interactive programme for three-dimensional visualization *SG3d* (GRASS4.1 Reference Manual 1993).

4.1. *Region in Central Illinois*

Regularized spline with tension and its derivatives were used for the computation of elevation, slope, and aspect raster maps with 2 m horizontal and 0·01 m vertical resolution from 10 foot contours digitized from a 1:24 000 topographic map. For the *smoothing* = 0·1 and *tension* = 20, the r.m.s deviation of the resulting surface was 0·39 m and the r.m.s crossvalidation error was 0·72 m, which was well within the accuracy of the original contour data, estimated as a half of the contour interval, in our case 1·52 m. Elevation and aspect were used for the construction of downhill flow lines with the computation of a raster map representing upslope contributing areas (figure 1), and for the construction of uphill flow lines with the computation of a raster map representing flow path lengths (figure 2). Results of topographic analysis were used for the computation of the *LS* factor for the standard form of USLE using equation (1) (figure 3), for the computation of the sediment transport

capacity index using equation (4) (figure 4) and for the location of areas with potential for erosion or deposition using equation (5) (figure 5).

The results demonstrate clearly why the USLE cannot be applied without previous localization and exclusion of areas with potential for deposition. The USLE predicts high erosion potential at the lower, concave parts of hillslopes, where deposition is usually observed. Because the influence of flow convergence is not included, the USLE predicts relatively low erosion in areas with convergent water flow and higher erosion in some areas with dispersal water flow (figure 3). The unit stream power based topographic index has significantly higher values in areas of water flow convergence (figure 4). The dramatic increase in sediment transport capacity in valleys that indicates the creation of channels is even more striking when the index T is visualized as a surface (figure 6).

The erosion/deposition index computed by equation (6) predicts high erosion

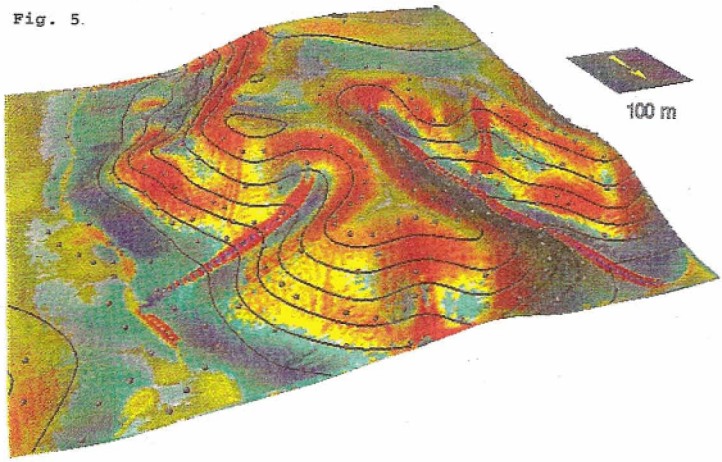

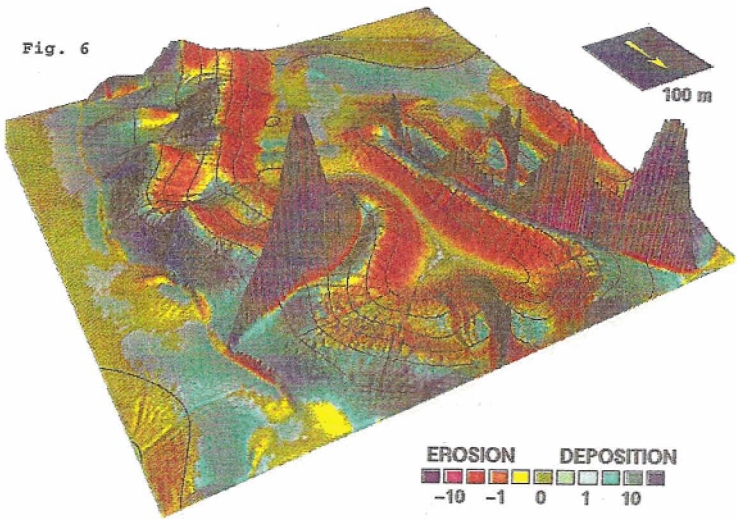

Figure 5. Topographic potential for erosion and deposition (gray points are the given data).

Figure 6. Topographic potential for erosion and deposition draped over surface representing sediment transport capacity.

potential in areas with profile convexity and tangential concavity with flow acceleration and convergence where water has the highest rate of potential energy dissipation (figure 5). High deposition potential is predicted in the areas with profile concavity with decreasing flow velocity (figure 5) which is in agreement with several published observations (Martz and de Jong 1987, Sutherland 1991, Busacca *et al.* 1993). Visualization of erosion/deposition potential as a colour map draped over the surface representing the sediment transport capacity (figure 6) shows that erosion potential is predicted in the areas with increase of sediment transport capacity, deposition potential in the areas of its decrease and zero potential is at the local extremas. This is in agreement with the description of the variation in erosion processes along complex slopes as presented by Foster (1990).

4.2. *Region in the Yakima Ridge*

For this region only the standard 30 m grid DEM was available. We have found the horizontal and vertical resolution, 30 m and 1 m respectively, insufficient for the analysis of water flow, and the results of topographic analysis using standard local polynomial interpolation were unacceptable (figure 9). To get reasonable results from these data we reinterpolated the elevations to a new DEM with 10 m horizontal and 0·01 m vertical resolution using regularized spline with tension, with simultaneous smoothing and computation of slope and aspect. Detailed analysis of the original and smoothed DEM, using three-dimensional shaded views, curvatures and histograms, revealed that two levels of systematic errors were significantly reduced—dense strips in the direction parallel to *y*-axis (see Mitasova *et al.* 1995) and less frequent strips in the north-western direction. The strong waves along the 20 m contour values, present in the original DEM, were also reduced but the profile curvature and histogram analysis revealed that it was not possible to remove the waves completely. Resampling and smoothing has improved the results for the upslope contributing areas (figure 7) and the sediment transport capacity index (figure 8). However, the erosion/deposition model still predicted waves of deposition along 20 m contours (figure 10). To confirm that these waves were artificial, we have extracted 10 m contours from the original grid DEM and interpolated a new DEM from these contours using our spline function with properly set smoothing and tension parameters. The new DEM has r.m.s deviation 2·3 m which is well within

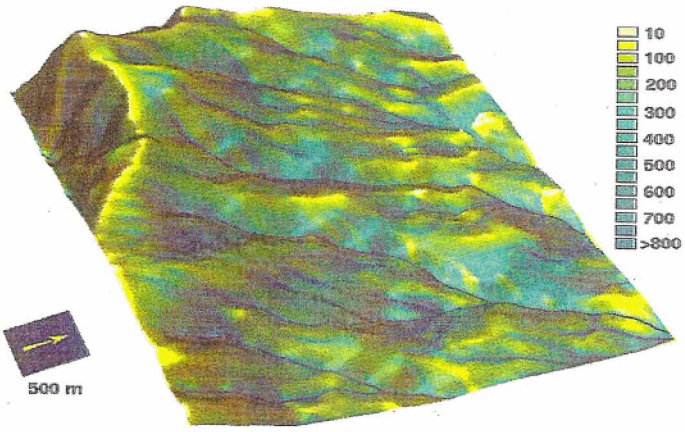

Figure 7. Upslope contributing areas computed from smoothed and resampled grid DEM.

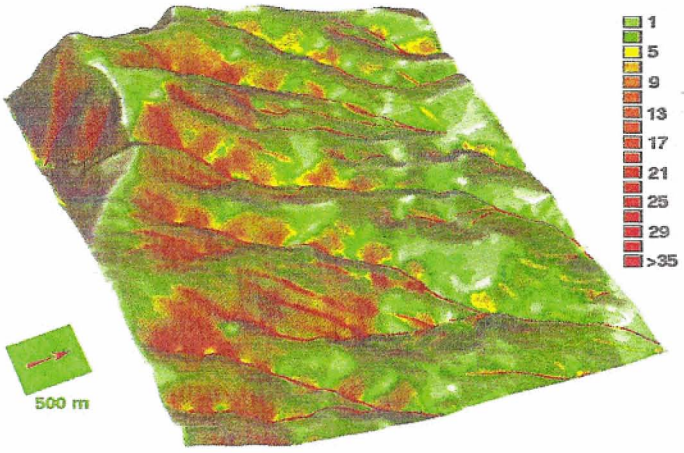

Figure 8. Sediment transport capacity index, computed from smoothed and resampled grid DEM.

the vertical accuracy of data (10 m), and the banding effect around each of the given contours is not present. The erosion/deposition model predicts the highest erosion in strongly convergent areas indicating creation of channels, and on the steep upper part of hillslope. Several depositional areas are predicted in concave parts of hillslope, mostly with dispersal flow.

Comparison of the results from the original, smoothed and recomputed DEMs (figures 9, 10, 11) demonstrates that the accuracy of the original USGS DEM was not sufficient for erosion/deposition modelling and more accurate data are needed to obtain reliable results.

5. Conclusions

Full integration of topographic analysis within a GIS, together with three-dimensional visualization, provided an environment for effective evaluation of various approaches to erosion/deposition risk assessment for landscape scale applications. The comparison of the USLE *LS* factor and the topographic erosion/deposition index demonstrated that the unit stream power based approach is more appropriate for landscape scale erosion modelling, especially when the location of both areas with erosion risk and with deposition potential is important. We have enhanced the unit stream power based approach by improving the computation of DEM using the smoothing spline with tension and by refining the flow tracing using the vector-grid algorithm. Originally proposed computation of the change in sediment transport capacity by finite difference technique was improved by using the directional derivatives of the bi-variate function representing the sediment transport capacity. Practical applications demonstrated that the digitized contours from 1:24 000 topographic map, used in the first example along with a reliable interpolation, were more suitable for erosion/deposition modelling than the standard 30 m DEM, which had insufficient resolution and several levels of systematic errors and artefacts.

Although the presented approach leads to the results in accordance with the observed spatial distribution of erosion and deposition in landscapes, reported in several papers (Sutherland 1991, Martz and de Jong 1992, Busacca *et al.* 1993, Suri and Hofierka 1994), its full validation using field measurements is still necessary, as

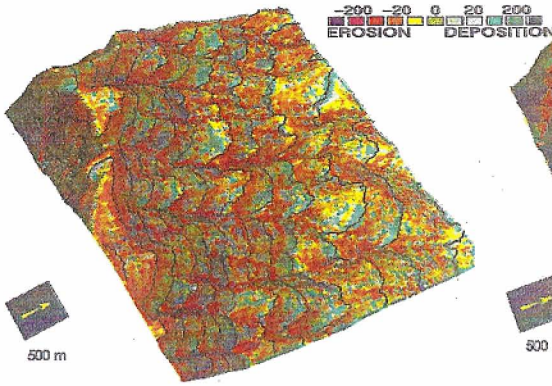

Fig.9

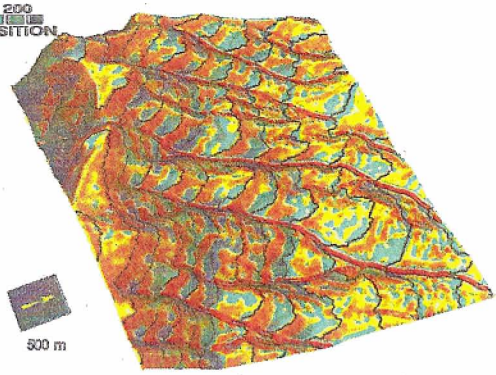

Fig.10

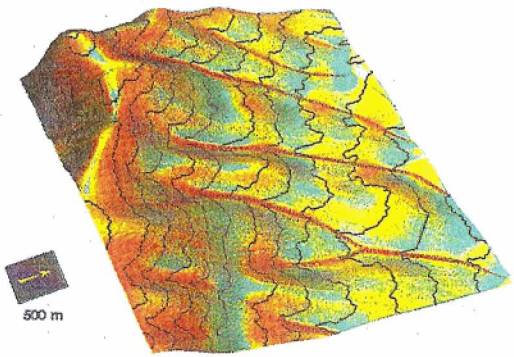

Fig.11

Figure 9. Topographic potential for erosion and deposition, computed from the original grid DEM.

Figure 10. Topographic potential for erosion and deposition, computed from smoothed and resampled grid DEM.

Figure 11. Topographic potential for erosion and deposition, computed from DEM interpolated from contours.

well as the estimation of the proper values of the m and n constants for different types of water erosion and terrain.

Acknowledgments

This research was funded in part by the City Water, Light and Power, Springfield, Illinois and by the DOD Strategic Environmental Research and Development Program (SERDP). This support is gratefully acknowledged. Stimulating discussions with Professor Ian D. Moore and Dr Michael Hutchinson from the Australian National University contributed to the development of presented methods. Comments by Dr Bahram Saghafian on hydrologic modelling and participation in the GRASS implementation and visualization by David Gerdes, Irina Kosinovsky and William Brown are also appreciated. We also thank anonymous reviewers for their valuable critiques of the manuscript.

Appendix

The regularized spline with tension and smoothing was used for interpolation from point data (in this case the digitized contours) to grid DEM, and for reinterpolat-

ing the existing grid DEM to higher resolution and reduction of its noise by smoothing. It was also used for the computation of first and second order partial derivatives for the estimation of slope and aspect and computation of directional derivatives of sediment transport capacity. The function has been derived by explicit minimization of a general smoothness functional (Mitas and Mitasova 1988, Mitasova and Mitas 1993), it includes tension and smoothing parameters and has regular derivatives of all orders. The interpolation function has the following form

$$F(x,y) = a_1 - \sum_{j=1}^{N} b_j \left\{ c_E + \ln\left[\left(\frac{r_j\phi}{2}\right)^2\right] + E_1\left[\left(\frac{r_j\phi}{2}\right)^2\right]\right\} \tag{A1}$$

where $r_j^2 = (x-x_j)^2 + (y-y_j)^2$ and $\{(x_j, y_j), j = 1,\ldots,N\}$ are the co-ordinates of given points, c_E is the Euler constant, E_1 is the exponential integral function, ϕ is the generalized tension parameter, and a_1, $\{b_j\}$ are the coefficients. The generalized tension parameter is used to tune the character of interpolant from thin steel plate to membrane and thus minimize the overshoots and artificial pits in the resulting digital elevation model. The unknown coefficients a_1, $\{b_j\}$ are found by solving the following system of linear equations

$$F(x_j, y_j) = z_j, \quad j = 1,\ldots,N \tag{A2}$$

$$\sum_{j=1}^{N} b_j = 0 \tag{A3}$$

If smoothing for the reduction of noise in data is desirable, then the equation (A2) is modified into the following form

$$F(x_j, y_j) + wb_j = z_j, \quad j = 1,\ldots,N \tag{A4}$$

where w is the smoothing parameter which controls the deviations of the resulting surface from the original data (Talmi and Gilat 1977, Wahba 1990). Smoothing was necessary both for the resampling of grid DEM to higher resolution and for the estimation of partial derivatives of surface representing sediment transport capacity.

Slope and aspect are computed directly from the partial derivatives of the function given by equation (A1), which have the following form

$$F_x = \frac{\partial F(x,y)}{\partial x} = \sum_{j=1}^{N} b_j R'(r_j)\frac{(x-x_j)}{r_j}, \quad F_y = \frac{\partial F(x,y)}{\partial y} = \sum_{j=1}^{N} b_j R'(r_j)\frac{(y-y_j)}{r_j} \tag{A5}$$

where

$$R'(r_j) = 2\frac{1-e^{-(\eta r_j)^2}}{r_j}, \quad \eta = \frac{\phi}{2} \tag{A6}$$

GRASS implementation of this function as *s.surf.tps* (GRASS4.1 Reference Manual) includes segmented processing based on quadtrees for applications to large data sets. As an option, simultaneously with interpolation, raster maps representing spatial distribution of slope, aspect, profile curvature, and tangential curvature are computed using the derivatives of the interpolation function (Mitasova and Hofierka 1993).

References

BUSACCA, A. J., COOK, C. A., and MULLA, D. J., 1993, Comparing landscape scale estimation of soil erosion in the Palouse using Cs-137 and RUSLE. *Journal of Soil and Water Conservation*, **48**, 361–367.

DOUGLAS, D. H., 1986, Experiments to locate ridges and channels to create a new type of digital elevation model. *Cartographica*, **23,** 29–61.

FLACKE, W., AUERSWALD, K., and NEUFANG, L., 1990, Combining a modified USLE with a digital terrain model for computing high resolution maps of soil loss resulting from rain wash. *Catena*, **17,** 383–397.

FAIRFIELD, J., and LEYMARIE, P., 1991, Drainage networks from grid digital elevation models. *Water Resources Research*, **27,** 709–717.

FOSTER, G. R., and WISCHMEIER, W. H., 1974, Evaluating irregular slopes for soil loss prediction. *Transactions of the American Society of Agricultural Engineers*, **12,** 305–309.

FOSTER, G. R., 1990, Process-based modelling of soil erosion by water on agricultural land. In *Soil Erosion on Agricultural Land*, edited by J. Boardman, I. D. L. Foster and J. A. Dearing (Chichester: John Wiley & Sons Ltd), pp. 429–445.

FREEMAN, T. G., 1991, Calculating catchment area with divergent flow based on regular grid. *Computers & Geosciences*, **17,** 413–422.

GARDNER, T. W., SASOWSKY, K. C., and RICK, L. D., 1990, Automated extraction of geomorphometric properties from digital elevation data, *Zeitschrift für Geomorphologie N.F.*, **Supplement-Bd80,** 57–68.

GRASS4.1 REFERENCE MANUAL, 1993, U.S. Army Corps of Engineers, Construction Engineering Research Laboratories, Champaign, Illinois, 422–425.

HOFIERKA, J., 1992, Interpolation, morphometric analysis of relief and modeling water erosion. M.S. thesis, Comenius University, Bratislava, Slovakia, 54. (in Slovak).

HUTCHINSON, M. F., 1989, A new procedure for gridding elevation and stream line data with automatic removal of spurious pits. *Journal of Hydrology*, **106,** 211–232.

HUANG, S. L., and FERNG, J. J., 1990, Applied land classification for surface water quality management: II. Land process classification. *Journal of Environmental Management*, **31,** 127–141.

JENSON, S. K., and DOMINGUE, J. O., 1988, Extracting topographic structure from digital elevation data for geographic information system analysis. *Photogrammetric Engineering and Remote Sensing*, **54,** 1593–1600.

JULIEN, P. Y., and SIMONS, D. B., 1985, Sediment transport capacity of overland flow. *Transactions of the American Society of Agricultural Engineers*, **28,** 755–762.

MARTZ, L. W., and JONG, E. DE, 1987, Using Cesium-137 to assess the variability of net soil erosion and its association with topography in a Canadian prairie landscape. *Catena*, **14,** 439–451.

MARTZ, L. W., and GARBRECHT, J., 1992, Numerical Definition of Drainage Network and Subcatchment Areas From Digital Elevation Models. *Computers & Geosciences*, **18,** 747–761.

MITASOVA, H., 1985, Cartographic Aspects of Computer Surface Modeling. PhD thesis, Slovak Technical University, Bratislava (in Slovak).

MITAS, L., and MITASOVA, H., 1988, General variational approach to the interpolation problem. *Computers and Mathematics with Applications*, **16,** 983–992.

MITASOVA, H., and IVERSON, L., 1992, Erosion and sedimentation potential analysis for Hunter lake. In *An environmental assessment of the Hunter Lake project area*, edited by W. U. Brigham, and A. R. Brigham (Champaign: Illinois Natural History Survey), pp. 1.2.01–08.

MITASOVA, H., AND MITAS, L., 1993, Interpolation by regularized spline with tension: I. Theory and implementation. *Mathematical Geology*, **25,** 641–655.

MITASOVA, H., and HOFIERKA, J., 1993, Interpolation by Regularized Spline with Tension II: Application to terrain modeling and surface geometry analysis. *Mathematical Geology*, **25,** 657–669.

MITASOVA, H., MITAS, L., BROWN, W. M., GERDES, D. P., KOSINOVSKY, I., and BAKER, T., 1995, Modeling spatially and temporally distributed phenomena: New methods and tools for GRASS GIS. *International Journal of Geographical Information Systems*, **9,** 433–446.

MOORE, I. D., and BURCH, G. J., 1986 a, Physical basis of the length-slope factor in the Universal Soil Loss Equation. *Soil Science Society of America Journal*, **50,** 1294–1298.

MOORE, I. D., and BURCH, G. J., 1986 b, Modeling erosion and deposition: Topographic effects. *Transactions American Society of Agricultural Engineers*, **29,** 1624–1640.

MOORE, I. D., and WILSON, J. P., 1992, Length-slope factors for the Revised Universal Soil Loss Equation: Simplified method of estimation. *Journal of Soil and Water Conservation*, **47**, 423–428.

PIKE, R. J., 1993, A bibliography of geomorphometry. Open-File Report 93-262-A, US Geological Survey, Menlo Park, California.

QIAN, J., EHRICH, R. W., and CAMPBELL, J. B., 1990, DNESYS—An expert system for automatic extraction of drainage networks from digital elevation data. *I.E.E.E. Transactions on Geoscience and Remote Sensing*, **28**, 29–44.

RENARD, G. K. FOSTER, G. R., WEESIES, G. A., and PORTER, J. P., 1991, RUSLE—Revised universal soil loss equation. *Journal of Soil and Water Conservation.* **46**, 30–33.

REWERTS, C. C. and ENGEL, B. A., 1991, ANSWERS on GRASS: Integrating a watershed simulation with a GIS. ASAE Paper No. 91-2621. American Society of Agricultural Engineers, St.Joseph, Missouri, 1–8.

ROO, A. P. J. DE, HAZELHOFF, L., and BURROUGH, P. A., 1989, Soil erosion modelling using 'ANSWERS' and Geographical information systems. *Earth Surface Processes and Landforms*, **14**, 517–532.

SRINIVASAN, R., and ENGEL, B. A., 1991, A knowledge based approach to extract input data from GIS, ASAE Paper No. 91-7045, American Society of Agricultural Engineers, St. Joseph, Missouri, 1–8.

SURI, M., and HOFIERKA, J., 1994, Soil water erosion identification using satellite and DTM data. In *Proceedings of the European Geographical Information Systems Conference (EGIS/MARI '94) (Utrecht: EGIS Foundation)*, 937–944.

SUTHERLAND, R. A., 1991, Caesium-137 and sediment budgeting within a partially closed drainage basin. *Zeitschrift für Geomorphologie*, **35**, 47–63.

TALMI, A., and GILAT, G., 1977, Method for Smooth Approximation of Data. *Journal of Computational Physics*, **23**, 93–123.

WAHBA, G., 1990, Spline models for observational data. *CNMS-NSF Regional Conference series in Applied Mathematics*, **59**, Society for Industrial and Applied Mathematics. Philadelphia, Pennsylvania.

WARREN, S. D., DIERSING, V. E., THOMPSON, P. J., and GORAN, W. D., 1989, An erosion-based land classification system for military installations. *Environmental Management*, **13**, 251–257.

WISCHMEIER, W. H., and SMITH, D. D., 1978, Predicting rainfall erosion losses, a guide to conservation planning. *Agriculture Handbook No. 537*, (Washington D.C., U.S. Department of Agriculture), 1–22.

ZHANG, W., and MONTGOMERY, D. R., 1994, Digital elevation model grid size, landscape representation and hydrologic simulations. *Water Resources Research*, **30**, 1019–1028.